

Published in final edited form as:

Ann Clin Transl Neurol. 2014 January 1; 1(1): 2–14. doi:10.1002/acn3.19.

Selective ROCK2 Inhibition In Focal Cerebral Ischemia

Jeong Hyun Lee, PhD^{1,2}, Yi Zheng, PhD^{1,2}, Daniel von Bornstadt, PhD¹, Ying Wei, MD¹, Aygul Balcioglu, PharmD, PhD¹, Ali Daneshmand, MD, MPH¹, Nilufer Yalcin, MD¹, Esther Yu, MS¹, Fanny Herisson, MD, PhD¹, Yahya B. Atalay, MD¹, Maya Hwewon Kim, BS¹, Yong-Joo Ahn, MD¹, Mustafa Balkaya, PhD¹, Paul Sweetnam, PhD³, Olivier Schueller, PhD³, Masha V. Poyurovsky, PhD⁴, Hyung-Hwan Kim, PhD¹, Eng H. Lo, PhD⁵, Karen L. Furie, MD⁶, and Cenk Ayata, MD^{1,7,*}

¹Neurovascular Research Laboratory, Department of Radiology, Massachusetts General Hospital, Harvard Medical School, Charlestown, MA 02129

³Surface Logix Inc, Brighton, MA 02135

⁴Kadmon Research Institute, New York, NY 10016

⁵Neuroprotection Research Laboratory, Department of Radiology, Massachusetts General Hospital, Harvard Medical School, Charlestown, MA 02129

⁶Department of Neurology, Rhode Island Hospital, Providence, RI 02903

⁷Stroke Service and Neuroscience Intensive Care Unit, Department of Neurology, Massachusetts General Hospital, Harvard Medical School, Boston, MA 02114

Abstract

Objective—Rho-associated kinase (ROCK) is a key regulator of numerous processes in multiple cell types relevant in stroke pathophysiology. ROCK inhibitors have improved outcome in experimental models of acute ischemic or hemorrhagic stroke. However, the relevant ROCK isoform (ROCK1 or ROCK2) in acute stroke is not known.

Methods—We characterized the pharmacodynamic and pharmacokinetic profile, and tested the efficacy and safety of a novel selective ROCK2 inhibitor KD025 (formerly SLx-2119) in focal cerebral ischemia models in mice.

Results—KD025 dose-dependently reduced infarct volume after transient middle cerebral artery occlusion. The therapeutic window was at least 3 hours from stroke onset, and the efficacy was sustained for at least 4 weeks. KD025 was at least as efficacious in aged, diabetic or female mice, as in normal adult males. Concurrent treatment with atorvastatin was safe, but not additive or synergistic. KD025 was also safe in a permanent ischemia model, albeit with diminished efficacy. As one mechanism of protection, KD025 improved cortical perfusion in a distal middle cerebral artery occlusion model, implicating enhanced collateral flow. Unlike isoform-nonselective ROCK inhibitors, KD025 did not cause significant hypotension, a dose-limiting side effect in acute ischemic stroke.

*Corresponding Author: Cenk Ayata, M.D.; Neurovascular Research Laboratory, Massachusetts General Hospital, 149 13th Street, Room 6403, Charlestown, MA 02129; Phone: (617) 726-8021; Fax: (617) 726-2547; cayata@partners.org.

²Current address: Division of Drug Discovery Research, Korea Research Institute of Chemical Technology, 141 Gajeongro, Yuseonggu, Daejeon 305-600, Korea

Author contributions: JHL, YZ, DvB, YW, AD, NY, EY, FH, MHK, YJA, MB, OS carried out the experiments and data analysis, CA designed the study, AB, PS, MVP, HHK, EHL, KLF and CA contributed to data analysis and manuscript preparation.

No conflict of interest exists.

Interpretation—Altogether, these data show that KD025 is efficacious and safe in acute focal cerebral ischemia in mice, implicating ROCK2 as the relevant isoform in acute ischemic stroke. Data suggest that selective ROCK2 inhibition has a favorable safety profile to facilitate clinical translation.

Introduction

Rho-associated protein kinase (ROCK) is an immediate downstream effector for Rho GTPases, and a key regulator of cytoskeletal dynamics, affecting numerous intracellular processes such as cell motility and contraction. Many of these cellular processes in vascular smooth muscle, endothelial cells, neurons, glia, leukocytes and platelets, are relevant to the pathophysiology of stroke, making ROCK a unique pleiotropic target with multiple potentially synergistic mechanisms against ischemic injury¹. ROCK has two isoforms that differ in their expression patterns in various tissues and cell types. Data suggest that ROCK2 is the predominant isoform expressed in neurons and vasculature²⁻⁴.

ROCK has been targeted in neurovascular diseases such as stroke for almost two decades. Small molecule ROCK inhibitors have vasodilator⁵, anti-aggregant⁶, and anti-inflammatory properties⁷, and reduce blood viscosity. ROCK inhibition has also been shown to preserve blood brain barrier⁸, suppress apoptotic cell death in penumbra⁹, induce a pro-survival phenotype in astrocytes¹⁰, and improve neuroplasticity and recovery after spinal cord injury^{11, 12}. Presumably a reflection of these converging mechanisms, ROCK inhibitors have been uniformly efficacious in various animal models of focal or global cerebral ischemia, and reduced hemorrhage rate after thrombolysis^{1, 13-15}. However, available inhibitors do not distinguish between the two isoforms, and can induce severe hypotension⁵ as a dose-limiting side effect that might compromise perfusion pressure and exacerbate ischemia in a subset of acute stroke patients.

Therefore, we systematically investigated the efficacy and safety of a novel ROCK2-selective inhibitor KD025 in rodent models of focal cerebral ischemia towards clinical translation. KD025 has 200-fold higher selectivity towards ROCK2 (IC₅₀ 105 nM) compared with ROCK1 (IC₅₀ 24 μM)¹⁶. Our results show that selective ROCK2 inhibition is at least as efficacious as previously published isoform-nonspecific inhibitors such as hydroxyfasudil, and has a favorable safety profile for clinical translation.

Methods

All experimental procedures were carried out in accordance with the Guide for Care and Use of Laboratory Animals (NIH Publication No. 85-23, 1996), and were approved by the institutional review board (MGH Subcommittee on Research Animal Care).

Study design

The clinical failure of many candidate drugs that showed promise in acute experimental ischemia underscores the importance of rigorous and comprehensive preclinical testing along published guidelines and recommendations by expert panels, including STAIR¹⁷⁻¹⁹ and ARRIVE²⁰. Therefore, we randomized and concealed allocation to treatment arms, reported all mortality as well as attrition due to other causes, and analyzed the data according to intention-to-treat principle and did not exclude animals showing signs of adverse effects such as vomiting or aspiration. Multiple experimenters blinded to the treatment group performed surgeries (JHL, YZ, YW, DvB) and assessed endpoints (MB, JHL, AD, YW, DvB, YZ). These experimenters did not administer the treatments as KD025 could be distinguished from the vehicle by its yellow color.

Animals and drug treatments

Young adult (C57BL/6J, 2-3 months old, male 22-30 g, female 16-23 g), aged (C57BL/6J, 12 months old, 33-52 g), or type 2 diabetic mice (db/db, B6.BKS(D)-*Lepr*^{db}/J, Jackson Laboratory; 2-3 months old, male, 33-50 g) were used in all experiments. Only one animal was excluded due to technical failure (hemorrhage during fMCAO in db/db mouse assigned to the vehicle group). KD025 (formerly SLx-2119) was kindly provided by Kadmon Corporation (New York, NY). Vehicle (0.4% methylcellulose) or KD025 (100, 200 or 300 mg/kg) was administered every 12 hour via orogastric gavage. The dosing paradigm was chosen based on the pharmacokinetic profile after oral administration in mice (see below). Atorvastatin (4 mg/mL) was dissolved in PBS (pH 7.4) containing 45% 3-hydroxypropyl- β -cyclodextrin and 10% ethanol, and administered at a dose of 20 mg/kg/d as a single daily intraperitoneal injection for 2 weeks as previously described²¹.

ROCK1 vs. ROCK2 selectivity

Recombinant ROCK1 and ROCK2 enzymes (truncated catalytic domains) were purchased from Invitrogen (#PV3691 and PV3759) and enzymatic activity was determined using [γ -³³P]ATP (5 mM) and S6 kinase substrate (17 mM). The reaction was run for 45 min at room temperature and was terminated by addition of phosphoric acid. [γ -³³P] phosphorylated S6 peptide was isolated by membrane filtration. The background was estimated by running the reaction in the absence of enzyme and radioactivity was assessed using a Microbeta Jet.

Pharmacokinetic studies

We measured plasma and brain concentrations of KD025 in male mice. Animals received 100 or 200 mg/kg KD025 twice a day for a total of 5 doses via orogastric gavage. Blood and brain tissue were collected at different time points after the last dose. For each time point, a different group of mice was sacrificed (n=5 each). Whole blood was collected via jugular vein into K₃EDTA tubes, and centrifuged at 3,000 rpm for 3 min at 4°C. Immediately following blood collection, mice were perfused with saline through the left ventricle to clear intravascular blood, and brains were harvested. All samples were stored at -80°C until analysis. Plasma and tissue KD025 concentrations were measured using high-resolution mass spectrometry (Thermo Fisher Q-Exactive; WIL Research Laboratories, Ashland, OH). Pharmacokinetic parameters were calculated using PKSolver²². A noncompartmental analysis was performed. The slope of the terminal log-linear part of the concentration versus time curve (λ_z) was calculated using the best-fit method. In addition, a one-compartmental analysis was performed for zero- or first-order kinetic models.

Recombinant ROCK1 and ROCK2 assays

Compound dilutions and reactions were performed in 96-well polystyrene low-binding plates. Filtration was done in 96-well filter plates containing hydrophilic phospho-cellulose cation exchanger membranes (Millipore). Enzymatic activity of the recombinant ROCK1 and ROCK2 (Invitrogen Corporation, Carlsbad, CA) was measured radiometrically in 50 μ l reaction mixture containing assay buffer (50 mM Tris, pH 7.5, 0.1 mM EGTA, 10 mM magnesium acetate and 1 mM DTT). Long S6 peptide (KEAKEKRQEIQAKRRRLSSLRASTSKSGGSQK, 30 μ M, America Peptide Company, Sunnyvale, CA), ROCK (4 mU per reaction) and ATP (10 μ M, Sigma-Aldrich; 1 μ Ci [γ -³³P]ATP, Perkin Elmer) and test compound were diluted to a final DMSO concentration of 1%. The reaction was incubated for 45 minutes at room temperature and stopped with 25 μ l 3% phosphoric acid. Phosphorylated long S6 peptide was separated from unreacted [γ -³³P]ATP by filtration of the quenched reaction contents through a P30 phosphocellulose filter plates using the Millipore Multiscreen® vacuum manifold system (Millipore, Bedford, MA). Each filter was washed 3 times with 75 μ l of 75 mM phosphoric acid and one time

with 30 μ l 100% methanol. Filter plates were allowed to dry and 30 μ l of OptiPhase 'SuperMix' scintillation fluid (Perkin Elmer) was added to each well.³³ Phosphorous was quantified in an I450 MicroBeta (Perkin Elmer) scintillation counter and corrected by subtracting the radioactivity associated with the background samples. Data were analyzed and expressed as percent inhibition using the formula $((U-B)/(C-B))*100$ where U is the unknown value, B is the average of staurosporine background wells and C is the average of control wells. Curve fitting was performed by GraphPad Prism software using sigmoidal dose-response (variable slope) equation type analysis to generate IC₅₀ values. K_i values were calculated from an equation of $K_i = IC_{50}/(1 + [S]/K_m)$, where [S] and K_m are the concentration of ATP and the K_m value of ATP, respectively²³.

Filament middle cerebral artery occlusion (fMCAO) and outcome assessments

Permanent or 1 hour transient fMCAO was induced in mice under isoflurane anesthesia (2.5% induction, 1.2% maintenance, in 70% N₂O/30% O₂)²⁴. Intraluminal filament (Doccol Corporation, Sharon, MA) was inserted through the external carotid artery. Mice were allowed to awaken from anesthesia after occlusion, and briefly re-anesthetized for filament removal in the transient ischemia group. Occlusion was confirmed using laser Doppler flowmetry (Perimed, OH) over the core MCA territory. Rectal temperature was controlled at 37°C by a servo controlled heating pad (FHC, CA) during the procedures. In all survival experiments, mice were placed in a temperature-controlled incubator with easy access to food and water after the procedure. Neurological deficits were assessed 48 hours after reperfusion, using five-point grading: 0, normal; 1, forepaw monoparesis; 2, circling to the left; 3, falling to the left; 4, no spontaneous walking and a depressed level of consciousness. At 48 hours after fMCAO, infarct areas were measured on ten 1 mm-thick 2,3,5-triphenyltetrazolium chloride (TTC)-stained coronal sections, integrated to calculate the infarct volume, and corrected for ischemic edema by subtracting the volume of ipsilateral non-infarcted tissue from the contralateral hemisphere. In addition, we assessed the incidence of hemorrhagic transformation on the same TTC-stained sections using a semi-quantitative grading system. In a separate group of mice, we assessed outcome at 4 weeks. To enhance long-term survival in this group, we administered intraperitoneal saline supplements (1 cc/day) and ampicillin (1 mg/day) for up to 7 days. Tissue outcome was quantified by measuring ipsilateral and contralateral hemispheric volumes and calculating tissue loss and atrophy using coronal cryosections. Neurological outcome was assessed weekly using the adhesive removal test, where the time (sec) to remove a sticky tape placed under the contralateral forepaw was quantified (maximum 180 sec)^{25, 26}.

Distal middle cerebral artery occlusion (dMCAO) and laser speckle-flowmetry

Mice (male, 25-30 g) were anesthetized with isoflurane as above, intubated and mechanically ventilated to maintain arterial pH and blood gas values within normal range, and femoral artery catheterized for continuous blood pressure monitoring and blood sampling (Table 1). Mice were then placed in a stereotaxic frame, a temporal burr hole (2 mm diameter) was drilled above the zygomatic arch, and middle cerebral artery was occluded just distal to the inferior cerebral vein using a microvascular clip. Cortical perfusion was imaged throughout the experiment using laser speckle flowmetry through intact skull²⁷. Cerebral blood flow (CBF) changes were calculated for each pixel relative to pre-ischemic baseline, and the area of cortex with residual CBF less than or equal to 20%, 21-30% and 31-40% was determined by thresholding.

Western Blotting

Whole mouse brains were collected at 36 and 72 hours after 1 hour fMCAO. Brain and heart were homogenized in lysis buffer (150 mM NaCl, 50 mM Tris pH 8.0, 0.5% NP-40, 50 mM

NaF, and 2 mM EDTA, protease inhibitor cocktail (Roche), HALT™ phosphatase inhibitor cocktail (Thermo Scientific) and incubated on ice 20-30 min. After centrifugation at 14,000g for 10 minutes at 4°C, the supernatant was collected. Protein concentration was determined with the Bio-Rad DC protein assay reagent (Bio-Rad, Hercules, CA). The protein lysates were separated on 4-15% SDS-PAGE and transferred onto nitrocellulose membrane. Blots were incubated with primary anti-p-MYPT1^{Thr696} (BD, San Diego, CA) antibody, followed by horseradish peroxidase-conjugated secondary antibody, and visualized by enhanced chemiluminescence reagents (ECL, Fisher Scientific, USA).

Statistical Analysis

Data were analyzed using Prism v 6.0b (GraphPad Software, San Diego, CA), and expressed as median with interquartile and full range (box and whisker plots) or mean ± standard error (SEM, line graphs, tables). Statistical methods and group sizes are given in figure legends. P<0.05 was considered statistically significant.

Results

ROCK1 vs. ROCK2 selectivity

KD025 selectively inhibited ROCK2 with IC₅₀ values approximately 60 nM, but had little effect on ROCK1 enzymatic activity at concentrations up to 10 μM in a recombinant enzyme system (Figure 1A). ROCK2 inhibition was competitive with ATP (Figure 1B). Table 1 shows the estimated K_i values of KD025 compared to the non-isoform selective inhibitors Y27632 and fasudil in ROCK activity assay. KD025 also inhibited ROCK activity in brain and heart when administered systemically, as measured by the degree of MYPT1^{Thr696} phosphorylation (Figure 1C).

Pharmacokinetic profile

To guide the dose and dose interval selection, we determined the pharmacokinetic profile of KD025 in mice. We administered the drug via orogastric gavage twice a day for 2 days and measured blood and brain tissue levels at predetermined time points starting immediately before the last dose at 48 hours (time 0; Figure 2). We used both non-compartmental analysis, and zero and first-order kinetic absorption models for one-compartmental analysis (Table 2). Plasma drug levels fitted better to the first-order absorption model (R²=0.98, Akaike Information Criterion [AIC]=8.31), whereas the brain drug levels fitted better to zero order absorption model (R²=0.98, AIC=6.52). Peak plasma and brain concentrations were reached within 2 hours of dosing, and exceeded the *in vitro* IC₅₀ by almost 10-fold. Brain exposure was approximately 5% of plasma exposure based on brain/plasma AUC ratio. Half-life was shorter in the brain than plasma (2 vs. 5 hours), presumably due to the higher elimination constant, distribution volume and clearance rate for the brain. Observed mean residence time was 4 and 7 hours for brain and plasma respectively, suggesting that the compound did not accumulate in the body at the dosing interval selected in this study (accumulation factor [R] 1.15 and 1.02 for plasma and brain, respectively). Nevertheless, 200 mg/kg dose level provided sustained plasma and tissue concentrations for at least 12 hours. Altogether, these data suggest that the selected dose levels and twice a day dosing paradigm were appropriate to test efficacy and safety in ischemia models.

Dose-response relationship

In initial experiments to determine the optimal dose, we started the treatment 24 hours before 1 hour transient fMCAO and continued until sacrifice at 48 hours (Figure 3). We found a U-shaped dose response relationship where 100 and 200 mg/kg dose levels reduced infarct volume by 30% and 40%, respectively. Efficacy was partially lost at 300 mg/kg dose

level, and we observed increased incidence of vomiting and respiratory difficulties presumably due to aspiration; these animals were nevertheless included in the analyses. At the optimal dose level of 200 mg/kg, infarct volume reduction was most prominent at middle to posterior coronal slice levels. Neurological deficits, crudely assessed using the 5-point scoring system prior to sacrifice, were also ameliorated. Based on these data, we used the optimal dose of 200 mg/kg in all subsequent experiments.

Ischemic tissue perfusion

We have previously shown that isoform-nonspecific ROCK inhibition acutely augments perfusion in ischemic tissue⁵. To test whether ROCK2 selective inhibitor KD025 shares this mechanism, we imaged the perfusion defect during dMCAO using laser speckle flowmetry non-invasively through intact skull. KD025 (200 mg/kg 90 min before dMCAO) significantly reduced the area of perfusion defect when compared with vehicle-treated animals (Figure 4). These data suggest that selective ROCK2 inhibition improves cortical perfusion during acute cerebral arterial occlusion, an effect shared with isoform-nonspecific ROCK inhibitors.

Therapeutic window of post-ischemic treatment

To determine the utility of KD025 as an acute stroke intervention, we next tested whether KD025 is efficacious when administered as a post-ischemic treatment alone. When administered starting 1 hour or 3 hours after the onset of fMCAO, KD025 (200 mg/kg) significantly reduced infarct volumes by 34% and 26%, respectively (Figure 5). Efficacy was completely lost if the treatment was started 6h after ischemia onset. Therefore, the therapeutic window of efficacy was at least 3 hours. In all subsequent experiments we tested the optimal efficacy time point of 1 hour after ischemia onset.

Long-term sustained efficacy

We next tested in a separate group of mice whether improved tissue outcome measured at 48 hours was sustained (Figure 6). Because accurate histological demarcation of infarcts at late time points is difficult, we used tissue loss and atrophy as an endpoint, calculated by measuring the ipsilateral and contralateral hemispheric volumes. KD025 (200 mg/kg twice a day for 36 hours starting 1 hour after ischemia onset) significantly reduced tissue loss in the ipsilateral hemisphere compared with vehicle when measured 4 weeks after ischemia. These data suggest that the beneficial effect of KD025 on tissue outcome is sustained into the subacute to chronic stage. Contralateral hemispheric atrophy as well as the neurological deficits also tended to be milder in the KD025 group, although these did not reach statistical significance.

Efficacy in female, aged or diabetic animals

Successful translation of stroke therapeutics critically depends on robust demonstration of efficacy in all clinically relevant cohorts. To this end, we tested KD025 in female and aged male mice, as well as in a mouse model of type 2 diabetes, a comorbid vascular risk factor common in stroke patients and associated with ROCK upregulation contributing to worse outcomes. Female mice developed overall smaller infarcts (Figure 7) compared with males (see Figures 3 and 5). KD025 appeared even more efficacious in females (42% reduction in infarct volume). Infarct volumes in aged males (12 months; Figure 7) were comparable to young animals (see Figures 3 and 5). KD025 reduced infarct volume by 34% compared with vehicle in aged mice. Type 2 diabetic *db/db* mice tended to develop larger infarct volumes (Figure 7) compared with age-matched wild type mice (Figures 3 and 5). KD025 reduced infarct volumes by 32% compared with vehicle in diabetic mice. These data suggest that KD025 maintains its efficacy in clinically relevant cohorts.

Safety in combination with statins

Statins inhibit ROCK signaling by reducing the synthesis of isoprenyl intermediates of cholesterol metabolism that are critical for Rho activation. This is believed to be responsible, at least in part, for the pleiotropic actions of statins. Therefore, KD025 may have additive or synergistic interactions with statins that may potentially be unsafe. We tested this in mice pretreated with atorvastatin (20 mg/kg/d) for 2 weeks. KD025 was safe in atorvastatin-pretreated mice, but did not show an additive or synergistic effect (Figure 8A).

Safety in permanent ischemia

Although most cerebral arterial occlusions eventually re-canalize, it is impossible to predict whether an occlusion will remain permanent in the hyperacute stage. If the drug were not safe in the absence of reperfusion, this would preclude its hyperacute administration in the field, adding to the delay in treatment initiation until imaging demonstration of recanalization. We, therefore, tested the safety of KD025 in permanent fMCAO. Because the model carries a high mortality over time, we assessed the infarct volume at 24 hours after ischemia onset to minimize excess losses. As expected, infarct volumes were larger in the permanent model (Figure 8B) compared to transient fMCAO (see Figures 3 and 5). KD025 was safe but lost its efficacy in the presence of persistent arterial occlusion.

Other safety endpoints

Hemorrhagic transformation, weight loss, and mortality were recorded in all experiments. None of these safety endpoints was significantly altered by KD025 in any of the experimental groups, except for increased weight loss when it was combined with atorvastatin (Table 3; Supplementary Figure 1). Because we did not have a sham group, it is unclear whether this increased weight loss is directly related to ischemia.

Systemic physiology

Previously tested isoform-nonspecific inhibitors cause hypotension that can be detrimental in acute stroke. Therefore, we tested the systemic physiological effects of the maximally efficacious KD025 dose level (200 mg/kg) in mice. Arterial blood pressures were only 8% lower in KD025 group compared with vehicle (Table 4), suggesting that the hypotensive effect of KD025 is much less potent than the previously tested isoform-nonspecific ROCK inhibitors⁵. Other systemic physiological parameters did not significantly differ between the groups.

Discussion

These data implicate for the first time ROCK2 as the relevant isoform in acute stroke. We found the novel ROCK2-selective small molecule inhibitor KD025 dose-dependently safe and efficacious in both males and females, with a therapeutic window of at least 3 hours. The effect size was comparable to previously published isoform-nonspecific inhibitors in similar animal models^{5, 14, 28}. Improved tissue outcomes persisted for at least 4 weeks, and were maintained in aged and diabetic animals. Moreover, the drug was safe in combination with a statin and in permanent ischemia, and unlike previously tested inhibitors, did not cause severe hypotension. It is, of course, possible that the dose-response and the therapeutic window, efficacy on long term outcome, and efficacy and safety in the permanent occlusion model may all be different in females, in comorbid animal models, and in combination with a statin. Unfortunately, testing all variables in all animal cohorts is not a feasible approach, and would have limited relevance in patient care, as the efficacy and safety profile would have to be characterized in clinical studies. Nevertheless, these data suggest that KD025 holds promise for rapid clinical translation in stroke. An intravenous formulation, if and

when available, may augment efficacy by rapidly achieving therapeutic plasma levels when administered in the hyperacute stage, although its hypotensive effect may also be stronger and dose-limiting.

Although ROCK2 is the main isoform expressed in the brain, predominantly in neurons^{2, 3, 29, 30}, both isoforms are also expressed in many other cell types relevant for acute stroke pathophysiology^{2, 3, 30-39}. For example, ROCK modulates endothelial nitric oxide synthase (eNOS) activity⁴⁰, and ROCK inhibitors acutely improve ischemic tissue perfusion in an eNOS-dependent manner^{5, 28}. ROCK2-selective KD025 also improved ischemic tissue perfusion in our study (Figure 3), and has been shown to mimic the effects of isoform-nonspecific inhibitors in endothelial migration assays⁴¹, suggesting that ROCK2 is the main target isoform in endothelial cells. Moreover, cerebral hypoxia and reoxygenation induces ROCK2 expression in microglia, and ROCK inhibitors suppress microglial inflammatory response and ameliorate injury in this model⁴². ROCK inhibition also suppresses leukocyte infiltration after ischemia, although ROCK1 may be the primary target for this effect^{15, 43, 44}. In platelets, ROCK promotes aggregation and thrombus contraction^{45, 46}, although not all studies agree¹³. Altogether, these data suggest that ROCK is a pleiotropic target acting through multiple independent mechanisms, and that brain penetration may not be a prerequisite for ROCK inhibitors to be neuroprotective in acute stroke. Nevertheless, our therapeutic paradigm achieved good brain tissue levels and target activity, which may be further enhanced upon ischemic blood-brain barrier disruption.

Hypotension is an important safety concern in acute stroke. Isoform-nonspecific ROCK inhibitors have acute and potent hypotensive effects that can be dose limiting in acute stroke, particularly if complete reperfusion has not been achieved^{5, 47}. KD025 induced only mild hypotension even at the maximally efficacious dose level, suggesting a more favorable safety profile. Indeed, the absence of hypotension probably allowed an even more potent improvement in perfusion by KD025 compared with isoform-nonspecific inhibitors⁵. Another potential safety concern is platelet inhibition, although an antithrombotic effect may in fact improve tissue perfusion in acute stroke as an additional mechanism of protection. Our semi-quantitative analysis did not detect an increase in the incidence of hemorrhagic transformation in the transient fMCAO model (Supplementary Figure 1), and ROCK inhibitors reportedly ameliorated tPA-induced hemorrhagic transformation in one study¹³.

Therapeutic time window is another important consideration in acute stroke therapy. Most if not all post-ischemic interventions gradually lose their efficacy as a function of time between stroke onset and treatment. In our studies, KD025 administered 1 hour after stroke onset was only marginally less efficacious than 24 hour pre-ischemic treatment. Indeed, the therapeutic window was between 3 and 6 hours, similar to tPA. While this is a relatively short time window for treatments that require vigorous screening prior to instituting the treatment (e.g. tPA), a drug with a favorable safety profile can easily be administered in the field thus markedly reducing the time to treatment. This was the case in Field Administration of Stroke Therapy-Magnesium (FAST-MAG) trial, where median treatment onset was 100 minutes after stroke onset and 70% of patients received treatment within 2 hours⁴⁸. KD025 showed no major side effects in one phase I study in healthy volunteers (Surface Logix, Brighton, MA), and the results of a subsequent extended dose range phase I study (Kadmon Corporation, New York, NY) are expected in the near future. It should also be noted that KD025 required 1 to 2 hours to reach the peak plasma levels after oral administration, suggesting that its therapeutic window for biological effect is even wider, and that an intravenous formulation can achieve efficacy even at later time points.

In summary, the novel ROCK2-selective kinase inhibitor KD025 showed good efficacy on cerebral ischemic outcome in multiple experimental cohorts with a therapeutic window and

safety profile favorable for rapid clinical translation. Future experiments will need to test safety in a second species, and in embolic MCAO with or without thrombolysis.

Supplementary Material

Refer to Web version on PubMed Central for supplementary material.

Acknowledgments

Supported by NIH (NS061505), The Heitman Foundation, and The Ellison Foundation. Study sponsors had no involvement in study design, data collection, analysis and interpretation, writing the report, or decision to publish.

References

1. Shin HK, Salomone S, Ayata C. Targeting cerebrovascular Rho-kinase in stroke. Expert opinion on therapeutic targets. 2008 Dec; 12(12):1547–64. [PubMed: 19007322]
2. Iizuka M, Kimura K, Wang S, et al. Distinct distribution and localization of Rho-kinase in mouse epithelial, muscle and neural tissues. Cell structure and function. 2012; 37(2):155–75. [PubMed: 22986902]
3. Nakagawa O, Fujisawa K, Ishizaki T, Saito Y, Nakao K, Narumiya S. ROCK-I and ROCK-II, two isoforms of Rho-associated coiled-coil forming protein serine/threonine kinase in mice. FEBS Lett. 1996 Aug 26; 392(2):189–93. [PubMed: 8772201]
4. Riento K, Ridley AJ. ROCKs: multifunctional kinases in cell behaviour. Nat Rev Mol Cell Biol. 2003 Jun; 4(6):446–56. [PubMed: 12778124]
5. Shin HK, Salomone S, Potts EM, et al. Rho-kinase inhibition acutely augments blood flow in focal cerebral ischemia via endothelial mechanisms. J Cereb Blood Flow Metab. 2007 May; 27(5):998–1009. [PubMed: 17033691]
6. Klages B, Brandt U, Simon MI, Schultz G, Offermanns S. Activation of G12/G13 results in shape change and Rho/Rho-kinase-mediated myosin light chain phosphorylation in mouse platelets. J Cell Biol. 1999 Feb 22; 144(4):745–54. [PubMed: 10037795]
7. Wang QM, Liao JK. ROCKs as immunomodulators of stroke. Expert opinion on therapeutic targets. 2012 Oct; 16(10):1013–25. [PubMed: 22925075]
8. Kahles T, Luedike P, Endres M, et al. NADPH oxidase plays a central role in blood-brain barrier damage in experimental stroke. Stroke. 2007 Nov; 38(11):3000–6. [PubMed: 17916764]
9. Wu J, Li J, Hu H, Liu P, Fang Y, Wu D. Rho-Kinase Inhibitor, Fasudil, Prevents Neuronal Apoptosis via the Akt Activation PTEN Inactivation in the Ischemic Penumbra of Rat Brain. Cell Mol Neurobiol. 2012 May 3.
10. Lau CL, Perreau VM, Chen MJ, et al. Transcriptomic profiling of astrocytes treated with the Rho kinase inhibitor Fasudil reveals cytoskeletal and pro-survival responses. Journal of cellular physiology. 2012 Mar; 227(3):1199–211. [PubMed: 21604263]
11. Lord-Fontaine S, Yang F, Diep Q, et al. Local inhibition of Rho signaling by cell-permeable recombinant protein BA-210 prevents secondary damage and promotes functional recovery following acute spinal cord injury. J Neurotrauma. 2008 Nov; 25(11):1309–22. [PubMed: 19061375]
12. Dergham P, Ellezam B, Essagian C, Avedissian H, Lubell WD, McKerracher L. Rho signaling pathway targeted to promote spinal cord repair. J Neurosci. 2002 Aug 1; 22(15):6570–7. [PubMed: 12151536]
13. Ishiguro M, Kawasaki K, Suzuki Y, et al. A Rho kinase (ROCK) inhibitor, fasudil, prevents matrix metalloproteinase-9-related hemorrhagic transformation in mice treated with tissue plasminogen activator. Neuroscience. 2012 Sep 18; 220:302–12. [PubMed: 22710066]
14. Koumura A, Hamanaka J, Kawasaki K, et al. Fasudil and ozagrel in combination show neuroprotective effects on cerebral infarction after murine middle cerebral artery occlusion. J Pharmacol Exp Ther. 2011 Jul; 338(1):337–44. [PubMed: 21493751]

15. Satoh S, Toshima Y, Hitomi A, Ikegaki I, Seto M, Asano T. Wide therapeutic time window for Rho-kinase inhibition therapy in ischemic brain damage in a rat cerebral thrombosis model. *Brain Res.* 2008 Feb 8.1193:102–8. [PubMed: 18187127]
16. Boerma M, Fu Q, Wang J, et al. Comparative gene expression profiling in three primary human cell lines after treatment with a novel inhibitor of Rho kinase or atorvastatin. *Blood Coagul Fibrinolysis.* 2008 Oct; 19(7):709–18. [PubMed: 18832915]
17. Fisher M, Feuerstein G, Howells DW, et al. Update of the stroke therapy academic industry roundtable preclinical recommendations. *Stroke.* 2009 Jun; 40(6):2244–50. [PubMed: 19246690]
18. Fisher M. Recommendations for advancing development of acute stroke therapies: Stroke Therapy Academic Industry Roundtable 3. *Stroke.* 2003 Jun; 34(6):1539–46. [PubMed: 12750546]
19. Recommendations for standards regarding preclinical neuroprotective and restorative drug development. *Stroke.* 1999 Dec; 30(12):2752–8. [PubMed: 10583007]
20. Kilkeny C, Browne WJ, Cuthill IC, Emerson M, Altman DG. Improving bioscience research reporting: the ARRIVE guidelines for reporting animal research. *PLoS biology.* 2010; 8(6):e1000412. [PubMed: 20613859]
21. Asahi M, Huang Z, Thomas S, et al. Protective effects of statins involving both eNOS and tPA in focal cerebral ischemia. *J Cereb Blood Flow Metab.* 2005 Jun; 25(6):722–9. [PubMed: 15716855]
22. Zhang Y, Huo M, Zhou J, Xie S. PKSolver: An add-in program for pharmacokinetic and pharmacodynamic data analysis in Microsoft Excel. *Computer methods and programs in biomedicine.* 2010 Sep; 99(3):306–14. [PubMed: 20176408]
23. Lin TS, Neenan JP, Cheng YC, Prusoff WH. Synthesis and antiviral activity of 5- and 5'-substituted thymidine analogs. *J Med Chem.* 1976 Apr; 19(4):495–8. [PubMed: 177781]
24. Eikermann-Haerter K, Hyun Lee J, Yuzawa I, et al. Migraine mutations increase stroke vulnerability by facilitating ischemic depolarizations. *Circulation.* 2012 Jan 17; 125(2):335–45. [PubMed: 22144569]
25. Balkaya M, Krober J, Gertz K, Peruzzaro S, Endres M. Characterization of long-term functional outcome in a murine model of mild brain ischemia. *J Neurosci Methods.* 2013 Mar 15; 213(2): 179–87. [PubMed: 23291083]
26. Freret T, Bouet V, Leconte C, et al. Behavioral deficits after distal focal cerebral ischemia in mice: Usefulness of adhesive removal test. *Behav Neurosci.* 2009 Feb; 123(1):224–30. [PubMed: 19170448]
27. Shin HK, Dunn AK, Jones PB, Boas DA, Moskowitz MA, Ayata C. Vasoconstrictive neurovascular coupling during focal ischemic depolarizations. *J Cereb Blood Flow Metab.* 2006 Aug; 26(8):1018–30. [PubMed: 16340958]
28. Rikitake Y, Kim HH, Huang Z, et al. Inhibition of Rho kinase (ROCK) leads to increased cerebral blood flow and stroke protection. *Stroke.* 2005 Oct; 36(10):2251–7. [PubMed: 16141422]
29. Duffy P, Schmandke A, Schmandke A, et al. Rho-associated kinase II (ROCKII) limits axonal growth after trauma within the adult mouse spinal cord. *J Neurosci.* 2009 Dec 2; 29(48):15266–76. [PubMed: 19955379]
30. Hashimoto R, Nakamura Y, Kosako H, et al. Distribution of Rho-kinase in the bovine brain. *Biochem Biophys Res Commun.* 1999 Sep 24; 263(2):575–9. [PubMed: 10491334]
31. Ishizaki T, Maekawa M, Fujisawa K, et al. The small GTP-binding protein Rho binds to and activates a 160 kDa Ser/Thr protein kinase homologous to myotonic dystrophy kinase. *Embo J.* 1996 Apr 15; 15(8):1885–93. [PubMed: 8617235]
32. Leung T, Chen XQ, Manser E, Lim L. The p160 RhoA-binding kinase ROK alpha is a member of a kinase family and is involved in the reorganization of the cytoskeleton. *Mol Cell Biol.* 1996 Oct; 16(10):5313–27. [PubMed: 8816443]
33. Miyagi Y, Carpenter RC, Meguro T, Parent AD, Zhang JH. Upregulation of rho A and rho kinase messenger RNAs in the basilar artery of a rat model of subarachnoid hemorrhage. *J Neurosurg.* 2000 Sep; 93(3):471–6. [PubMed: 10969946]
34. Wei, L.; Roberts, W.; Wang, L., et al. *Development.* Vol. 128. Cambridge, England: 2001 Aug. Rho kinases play an obligatory role in vertebrate embryonic organogenesis; p. 2953-62.

35. Matsui T, Amano M, Yamamoto T, et al. Rho-associated kinase, a novel serine/threonine kinase, as a putative target for small GTP binding protein Rho. *Embo J*. 1996 May 1; 15(9):2208–16. [PubMed: 8641286]
36. Noma K, Rikitake Y, Oyama N, et al. ROCK1 mediates leukocyte recruitment and neointima formation following vascular injury. *J Clin Invest*. 2008 May; 118(5):1632–44. [PubMed: 18414683]
37. Zhang YM, Bo J, Taffet GE, et al. Targeted deletion of ROCK1 protects the heart against pressure overload by inhibiting reactive fibrosis. *Faseb J*. 2006 May; 20(7):916–25. [PubMed: 16675849]
38. Rikitake Y, Oyama N, Wang CY, et al. Decreased perivascular fibrosis but not cardiac hypertrophy in ROCK1^{+/-} haploinsufficient mice. *Circulation*. 2005 Nov 8; 112(19):2959–65. [PubMed: 16260635]
39. Schueller O, Tong W, Ferkany J, Sweetnam P. Selective ROCK 2 Inhibition Attenuates Arterial Plaque Formation in an ApoE Knockout Mouse Model. *Circulation*. 2006:228. [PubMed: 17190865]
40. Noma K, Oyama N, Liao JK. Physiological role of ROCKs in the cardiovascular system. *Am J Physiol Cell Physiol*. 2006 Mar; 290(3):C661–8. [PubMed: 16469861]
41. Breyer J, Samarin J, Rehm M, Lautscham L, Fabry B, Goppelt-Struebe M. Inhibition of Rho kinases increases directional motility of microvascular endothelial cells. *Biochem Pharmacol*. 2012 Mar 1; 83(5):616–26. [PubMed: 22192821]
42. Ding J, Li QY, Wang X, Sun CH, Lu CZ, Xiao BG. Fasudil protects hippocampal neurons against hypoxia-reoxygenation injury by suppressing microglial inflammatory responses in mice. *J Neurochem*. 2010 Sep; 114(6):1619–29. [PubMed: 20882700]
43. Satoh S, Kobayashi T, Hitomi A, et al. Inhibition of neutrophil migration by a protein kinase inhibitor for the treatment of ischemic brain infarction. *Jpn J Pharmacol*. 1999 May; 80(1):41–8. [PubMed: 10446755]
44. Satoh S, Utsunomiya T, Tsurui K, et al. Pharmacological profile of hydroxy fasudil as a selective rho kinase inhibitor on ischemic brain damage. *Life Sci*. 2001 Aug 10; 69(12):1441–53. [PubMed: 11531167]
45. Yang SA, Carpenter CL, Abrams CS. Rho and Rho-kinase mediate thrombin-induced phosphatidylinositol 4-phosphate 5-kinase trafficking in platelets. *J Biol Chem*. 2004 Oct 1; 279(40):42331–6. [PubMed: 15277528]
46. Ono A, Westein E, Hsiao S, et al. Identification of a fibrin-independent platelet contractile mechanism regulating primary hemostasis and thrombus growth. *Blood*. 2008 Jul 1; 112(1):90–9. [PubMed: 18310501]
47. Kast R, Schirok H, Figueroa-Perez S, et al. Cardiovascular effects of a novel potent and highly selective azaindole-based inhibitor of Rho-kinase. *Br J Pharmacol*. 2007 Dec; 152(7):1070–80. [PubMed: 17934515]
48. Saver JL, Kidwell C, Eckstein M, Starkman S. Prehospital neuroprotective therapy for acute stroke: results of the Field Administration of Stroke Therapy-Magnesium (FAST-MAG) pilot trial. *Stroke*. 2004 May; 35(5):e106–8. [PubMed: 15017009]

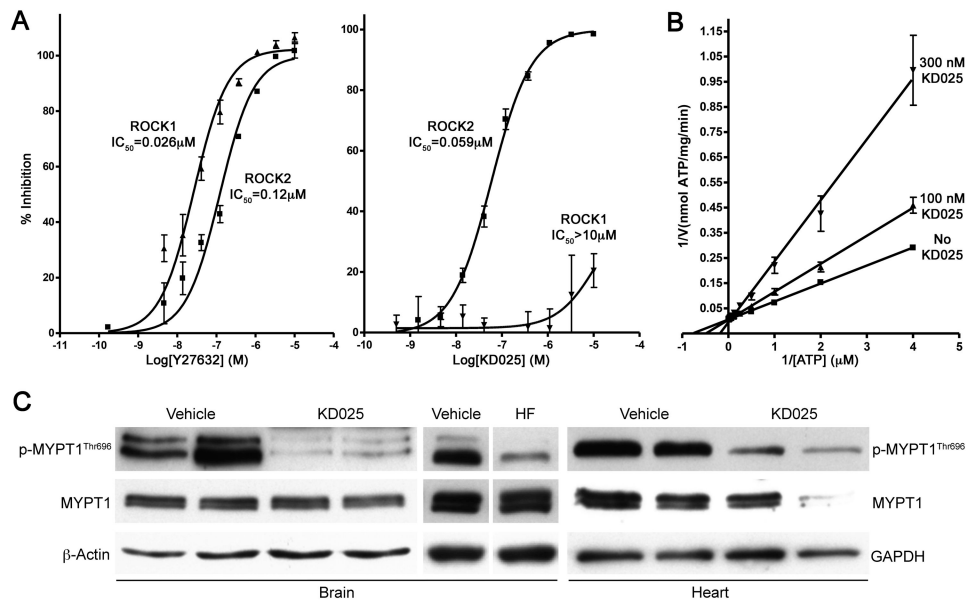


Figure 1. ROCK1 vs. ROCK2 selectivity, *in vitro*

(A) KD025 selectively inhibited ROCK2 over ROCK1, whereas isoform nonselective Y27632 inhibited ROCK1 and ROCK2 to a similar extent in a recombinant enzyme system with truncated catalytic domains. IC_{50} values for each drug are indicated on the graphs.

(B) ROCK2 inhibition by KD025 was competitive with ATP.

(C) Systemic administration of KD025 (200 mg/kg via oral gavage 1 hour before harvesting the tissues) inhibited ROCK activity in the brain, as well as in the heart and aorta, as measured by MYPT1 phosphorylation in mice ($n=2$ each vehicle and KD025). Total MYPT1 levels did not show a consistent change. The effect was comparable to that of isoform non-selective ROCK inhibitor hydroxyfasudil (HF, 10 mg/kg, intraperitoneal).

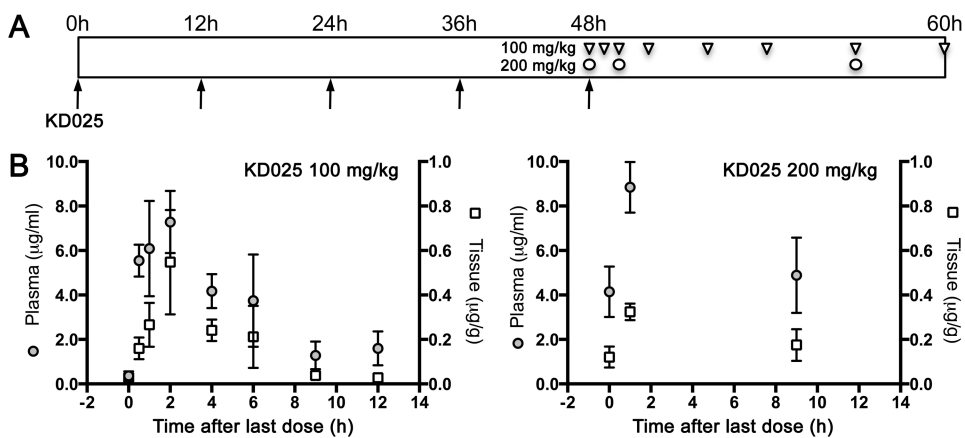


Figure 2. Pharmacokinetic analysis

(A) KD025, 100 or 200 mg/kg, was administered (arrows) via oral gavage every 12 hours for 48 hours (5 doses). Plasma and tissue samples were collected at 0, 1, 2, 4, 6, 9 and 12 hours after the last 100 mg/kg dose (triangles), and at 0, 2 and 9 hours after the last 200 mg/kg dose (circles) ($n=5$ mice for each time point and dose level). Note that only a subset of time points were studied at the higher dose level.

(B) Plasma (circles) and brain tissue (squares) KD025 concentrations are shown at 100 mg/kg (left panel) or 200 mg/kg (right panel) dose levels. Mean \pm SEM.

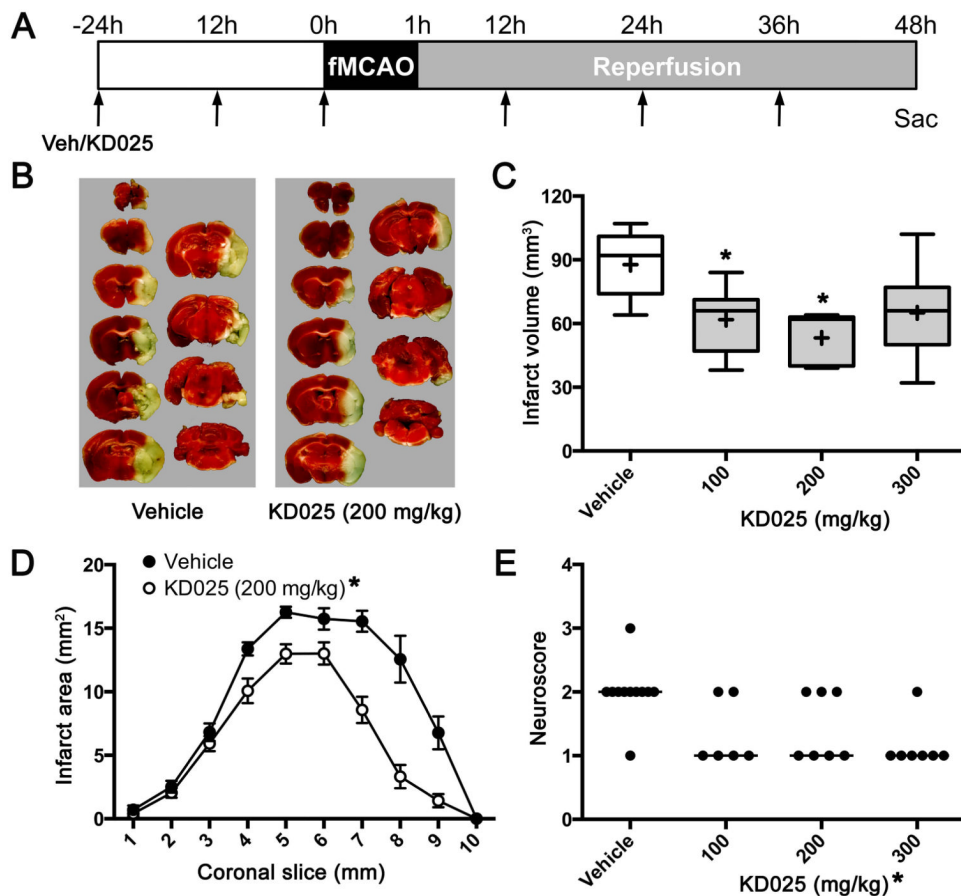


Figure 3. Dose-response relationship

(A) Vehicle or KD025 was administered (arrows) every 12 hours starting 24 hours before the onset of 1 hour transient fMCAO and continued until sacrifice at 48 hours (6 doses). (B) Representative TTC-stained 1 mm-thick coronal brain slices show the infarct in vehicle- or KD025-treated mice. (C) Infarct volumes (indirect method) were significantly smaller after 100 or 200 mg/kg KD025 (n=6 and 7, respectively) compared with vehicle (n=11). The effect was partially lost at 300 mg/kg dose level (n=7). *p<0.05 vs. vehicle. Boxes, median and interquartile range; whiskers, min-max; +, mean. One-way ANOVA followed by Dunnett's multiple comparisons test. (D) Infarct areas were smaller at middle and posterior coronal slice levels (1 mm-thick) in KD025 (200 mg/kg) group compared with vehicle (n=7 and 11, respectively). *p<0.05 vs. vehicle. Mean±SEM. Two-way ANOVA followed by Sidak's multiple comparisons test. (E) Neurological deficits were milder in KD025-treated groups compared with vehicle when assessed at 48 hours (see Methods for scoring system). *p<0.05 vs. vehicle. Kruskal-Wallis test.

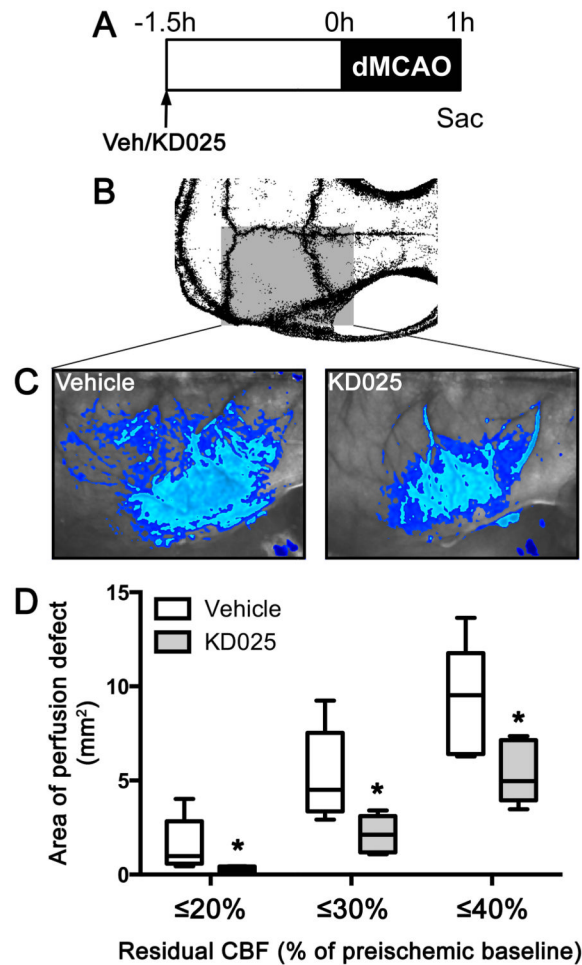


Figure 4. Perfusion deficit

(A) Vehicle or KD025 (200 mg/kg via orogastric gavage) was administered (arrow) 90 min before dMCAO.

(B) Position of laser speckle imaging field is shown covering the entire right hemisphere.

(C) Laser speckle blood flow maps show representative perfusion defects in vehicle- or KD025-treated mice. Regions with <30% (light blue) or 31-40% (dark blue) residual blood flow are shown (see Methods for details). Clip artifact is seen on the lower right of each image.

(D) Area of cortical perfusion defect was smaller in KD025 group compared with vehicle at all thresholding levels (n=5 each). *p<0.05 vs. vehicle. Boxes, median and interquartile range; whiskers, min-max. Two-way ANOVA followed by Sidak's multiple comparisons test.

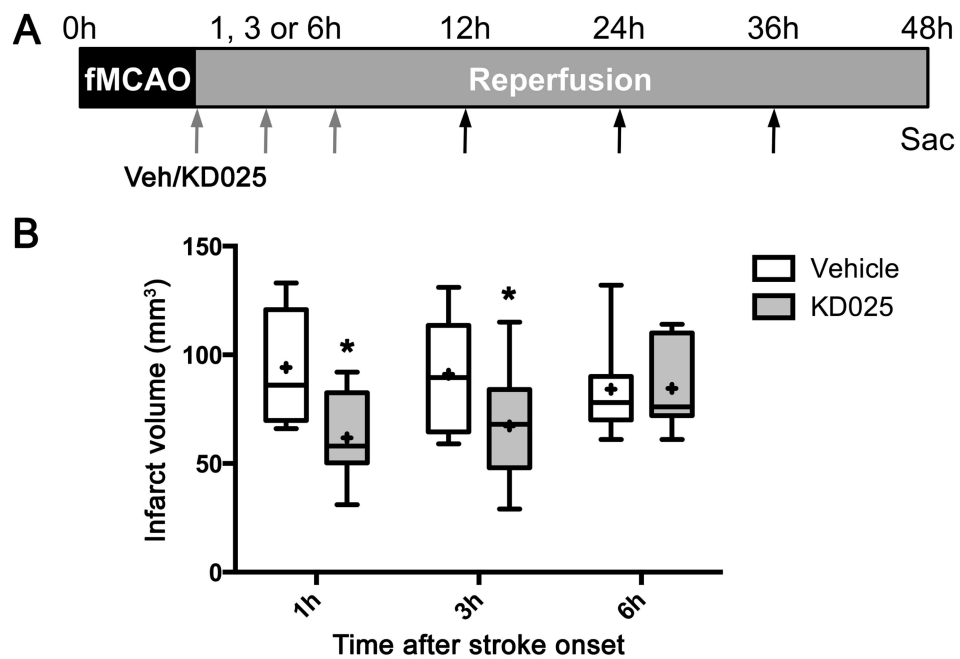


Figure 5. Therapeutic window

(A) Vehicle or KD025 was administered (arrows) starting 1, 3 or 6 hours after fMCAO and continued until sacrifice at 48 hours (4 doses).

(B) Infarct volumes (indirect method) are shown after post-ischemic vehicle or KD025 (200 mg/kg) treatment starting 1, 3 or 6 hours after dMCAO. KD025 was efficacious when administered 1 or 3 hours but not 6 hours after stroke onset (n=8, 14, 7 vehicle, and 8, 15, 7 KD025, at 1h, 3h and 6h time points, respectively). *p<0.05 vs. vehicle. Boxes, median and interquartile range; whiskers, min-max; +, mean. Two-way ANOVA followed by Sidak's multiple comparisons test.

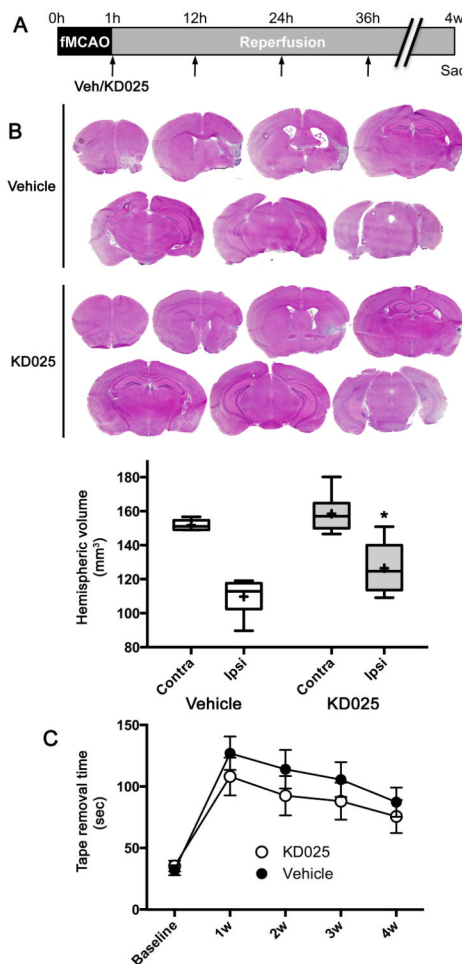


Figure 6. Long term tissue and neurological outcome

(A) Vehicle or KD025 was administered (arrows) starting 1 hour after fMCAO for a total of 4 doses, followed by tissue outcome assessment at 4 weeks.

(B) Representative hematoxylin/eosin-stained coronal cryosections and ipsilateral and contralateral hemispheric volumes show tissue loss and atrophy at 4 weeks after stroke in vehicle- or KD025-treated mice (n=6 and 9, respectively). Substantial atrophy was present in ipsilateral hemisphere compared with contralateral. KD025 reduced the amount of tissue loss. * $p < 0.05$ vs. vehicle. Boxes, median and interquartile range; whiskers, min-max; +, mean. Two-way ANOVA followed by Sidak's multiple comparisons test.

(C) The improvement in neurological function, assessed by the time to remove an adhesive tape from the contralateral forepaw, did not reach statistical significance between vehicle- and KD025-treated mice (n=17 each). Mean \pm SEM. Two-way ANOVA for repeated measures.

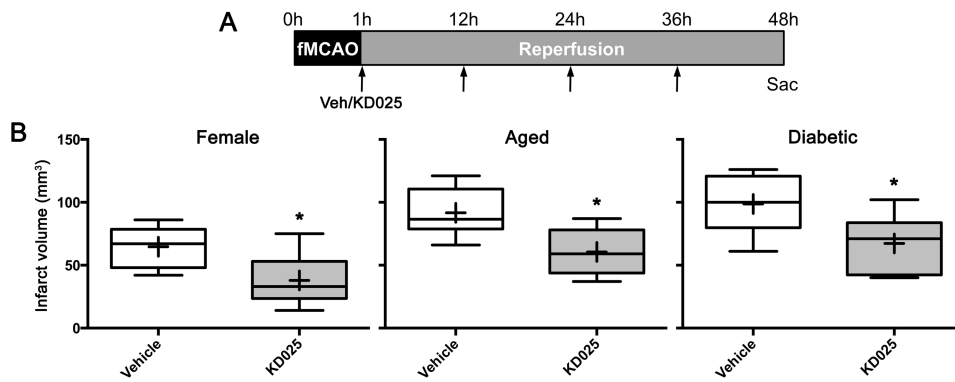


Figure 7. Efficacy in female, aged and diabetic mice

(A) Vehicle or KD025 administration (arrows) was started 1 hour after fMCAO and continued until tissue outcome assessment at 48 hours (4 doses).

(B) Infarct volumes (indirect method) after vehicle or KD025 (200 mg/kg) in female (n=9 each), aged (12 months; n=6 each) and diabetic (db/db) mice (n=6 and 8, respectively). One db/db mouse in the vehicle group was excluded at the time of surgery due to technical failure. * $p < 0.05$ vs. vehicle. Boxes, median and interquartile range; whiskers, min-max; +, mean. Unpaired t-test.

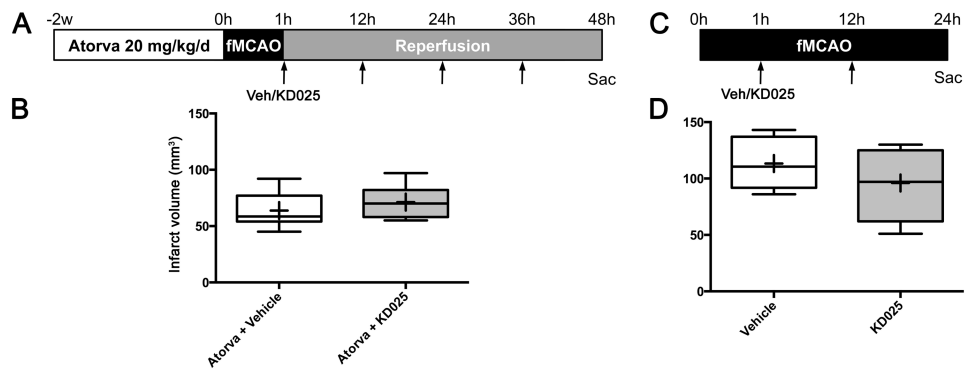


Figure 8. Safety in combination with atorvastatin and in permanent ischemia

(A) Daily atorvastatin treatment for 2 weeks was followed by vehicle or KD025 administration (arrows) starting 1 hour after fMCAO and continuing until sacrifice for tissue outcome assessment at 48 hours (4 doses).

(B) Infarct volumes (indirect method) after vehicle or KD025 (200 mg/kg) in combination with atorvastatin (n=6 each). Boxes, median and interquartile range; whiskers, min-max; +, mean. Unpaired t-test.

(C) Timeline shows vehicle or KD025 administration (arrows) via oral gavage starting 1 hour after permanent fMCAO and continuing until tissue outcome assessment at 24 hours (2 doses).

(D) Infarct volumes (indirect method) in vehicle or KD025 (200 mg/kg) groups after permanent fMCAO (n=10 and 9, respectively; p=0.19). Boxes, median and interquartile range; whiskers, min-max; +, mean. Unpaired t-test.

Table 1
ROCK1 vs. ROCK2 selectivity of KD025 in comparison with Y27632 and fasudil

	KD025	Y27632	Fasudil
ROCK2 K _i (nM)	41 ± 2	77 ± 5	112 ± 8
ROCK1 K _i (nM)	>10,000	68 ± 2	145 ± 7

Table 2
Pharmacokinetic (PK) parameters at 100 mg/kg KD025 dose level

		Plasma	Brain
Non-compartmental analysis	AUC _{inf} (h*µg/ml)	51.93	2.37
	CL (L/h)	1.93	-
	MRT (h)	6.81	4.17
	V (L)	11.58	-
	λ ₂ (1/h)	0.16	0.31
	T _{1/2} (h)	4.16	2.21
	AUC _{last} (h*µg/ml)	42.31	2.28
	T _{max} (h)	2	2
	C _{max} (µg/ml)	7.28	0.54
One-compartment first-order kinetic absorption model	AUC _{inf} (h*µg/ml)	44.83	2.05
	CL (L/h)	2.23	-
	V (L)	11.90	-
	k _a (1/h)	2.23	-
	k _e (1/h)	0.18	0.32
	A (µg/ml)	9.16	0.67
	T _{1/2} (h)	3.69	2.12
	T _{max} (h)	1.21	2
MRT (h)	5.78	3.06	

AUC, area under the concentration vs time curve; AUC_{inf}, AUC until infinity; CL, total body clearance; MRT, mean residence time; V, volume of distribution; K_a, absorption rate constant; K_e, elimination rate constant; A, absorption; λ₂, slope of the log-linear terminal phase; T_{1/2}, half-life; AUC_{last}, AUC until last measurement time point; T_{max}, time to maximum concentration; C_{max}, maximum concentration.

Table 3
Safety endpoints

Experiment	Treatment onset	Dose level (mg/kg)	Weight loss (g)	Mortality
Dose response	24h pre-ischemic	Vehicle	5.3 ± 0.5	0/6
		100	4.3 ± 0.6	0/6
		200	3.5 ± 0.4	1/8
		300	4.5 ± 0.5	2/9
Therapeutic window	1-6h post-ischemic	Vehicle	4.9 ± 0.3	1/30
	1h post-ischemic	200	5.7 ± 0.2	1/9
	3h post-ischemic	200	5.2 ± 0.2	0/15
	6h post-ischemic	200	5.6 ± 0.3	1/8
Female	1h post-ischemic	Vehicle	2.9 ± 0.5	0/9
		200	3.5 ± 0.4	0/9
Aged (12 mo)	1h post-ischemic	Vehicle	4.2 ± 0.7	1/7
		200	3.4 ± 0.6	2/8
Diabetic (db/db)	1h post-ischemic	Vehicle	3.8 ± 0.3	0/6
		200	3.8 ± 0.3	0/8
Atorvastatin (20 mg/kg)	1h post-ischemic	Vehicle	3.3 ± 0.8	1/7
		200	5.7 ± 0.3*	1/7
Permanent ischemia	1h post-ischemic	Vehicle	4.0 ± 0.3	2/12
		200	3.5 ± 0.3	6/15

All treatments were administered every 12h via oral gavage until sacrifice at 48h (24h in permanent ischemia experiment). Please see methods and results for details of experimental groups and protocols, and the treatment paradigms. Weight loss expressed as mean±SEM.

* p<0.05 vs. atorvastatin plus vehicle. Unpaired t-test or one-way ANOVA for weight loss, chi-square or Fisher's exact test for mortality.

Table 4

Systemic physiological parameters

	BP (mmHg)	HR (bpm)	pH	pCO ₂ (mmHg)	pO ₂ (mmHg)
Vehicle	84 ± 1	571 ± 32	7.34 ± 0.01	33 ± 2	135 ± 10
KD025 (200 mg/kg)	77 ± 3*	618 ± 19	7.36 ± 0.02	29 ± 2	135 ± 13

* p=0.06 vs. vehicle. Unpaired t-test. Mean±SEM.